Experimental Characterization of Piezoelectric Transducers for Automotive Composite Structural Health Monitoring

Experimental Characterization of Piezoelectric Transducers for Automotive Composite Structural Health Monitoring

Massimiliana Carello, Alessandro Ferraris, Andrea Giancarlo Airale, Alessandro Messana, Lorenzo Sisca,

Henrique de Carvalho Pinheiro, and Simone Reitano

Politecnico di Torino

Abstract

Composite materials are a natural choice for automotive applications where mechanical performance and lightweight are required. Nevertheless, attention should be directed to the defects into the material. This paper presents the building up of a Structural Health Monitoring system based on a piezoelectric transducers network: a continuous data system acquisition has been carried out in order to detect the presence of faults inside the analyzed structure. A piezoceramic patch has been coupled to a host structure in composite, to characterize the acquisition and the transmission of a wave signal on the material. The importance of this advanced technology research and the positive results obtained in the case study constitute the starting point for future application of piezoelectric-based Structural Health Monitoring systems over real industrial components.

Introduction

Nowadays, a lot of engineering applications are focused on lightweight design for a wide range of components. Consequently, composite materials, thanks to their high stiffness to mass ratio and customizable design and according to specific requested properties, become the first choice in setting up new projects [1-3]. Despite of the great advantages that come from the composite materials usage for a wide range of application, some drawbacks must be considered and highlighted: first, the lack of experience and knowledge in practical applications in comparison with the traditional metallic structures, for example the NVH behavior [4-8]; second, the complex understanding for damage formation or its detection [9]. All that makes the health condition assessment for a composite structure hard to accomplish. In this field, the SHM technique [10] stands as a promising development. The continuous data acquisition regarding the health status of a host structure and the constant analysis of the stored signals are the main features of the monitoring method. A sensors network, permanently bonded to the host structure in order to create a non-destructive test system that could be considered as an integral part of the overall structure, performs the data collection. All the processed data are employed to define a decisional procedure that assesses the structure ability to fulfil its mission, for nominal conditions. The SHM, already used in the civil field for the infrastructures monitoring [11,12] and in the aerospace field for the metallic structures [13-15], is discovering particular interest for the composite application [16-20]. Figure 1 shows a schematic representation of the main steps that allow the structural health monitoring.

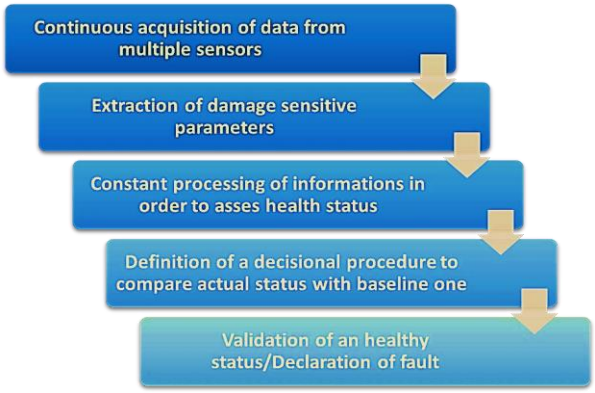

Figure 1: Schematic steps for a Structural Health Monitoring system.

The real-time and the remote monitoring of the host structure health status not only increases the overall safety condition, but also allows to identify the damage creation at the occurrence, without the necessity to wait until the next scheduled maintenance. In addition, the ability to offer a continuative data acquisition, after the defect appearance, helps to find out at the root the causes of a failure, and to gain experience-improving design to avoid it. The massive quantity of data recorded helps to build an empirical database that defines a statistical behaviour for the material. This information becomes essential for the composite materials, where the specific certification absence makes conventional the safety coefficient

definition based on empirical constructor know-how. A composite structure monitoring for a long period with a continuous sampling allows the detection of unexpected damage after collision and helps the determination of the fatigue limit.
In summary, SHM allows to pass from estimated usage pattern to a knowledge of the actual utilization.
If a good accuracy in detection is certified, a SHM method could also reduce the downtime required for maintenance, because of the easier and faster procedure requested in respect of classical NDT methods, such as visual inspections, ultrasonic C-scan, thermography or radiography. Furthermore, the possibility to automatize the process with a minimum control needed by the user, could avoid errors generated by human factor (like tiredness or negligence). Figure 2 shows a qualitative example of comparison between structures with and without SHM regarding reliability and costs [10].
Piezoceramic transducers are massively used to perform SHM in the aerospace industry. Table 1 shows an estimation of inspection time that could be saved on a flight line thanks to a permanent SHM system [16].

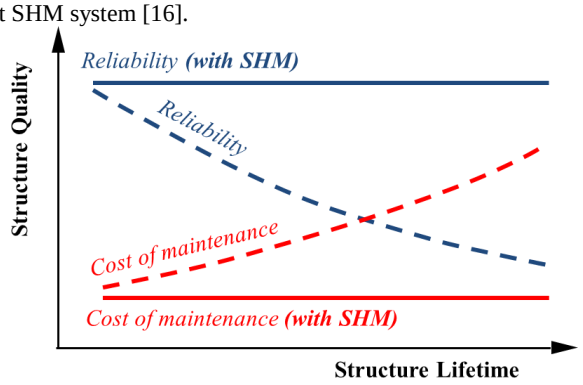

Figure 2: SHM advantages in terms of reliability and cost of maintenance on the host structure [10].

Table 1: Investigation about time saved with an SHM system in respect of a classical NDT maintenance [16].

Inspection type	Actual inspection time (% of total)	Saved inspection time (% of total)	Estimated potential for smart systems (%)
Flight line	*16*	*6*	*-40*
Scheduled	*31*	*14*	*-45*
Unscheduled	*16*	*2*	*-10*
Service instructions	*37*	*22*	*-60*
Total	***100***	***44***	***-44***

The requirements of lightweight, low cost, wide range of applicability and easy coupling with host structure are perfectly fitted. In addition, the possibility for each piezo patch to act as a sensor or an actuator allows:

- Passive monitoring: the host structure deformations induce a signal to the piezo sensors, from which is obtained a sensitive damage index. Depending on the specific parameter monitored, different fault detection algorithm can be implemented.
- Active/passive monitoring: the piezo actuators ability to excite the host structure is used. A reference status for the healthy structure is recorded, and step-by-step compared with the real time acquisition of the piezo sensors, to give a damage index.

Rytter [12] classifies the damage definition in four levels of information that a SHM system must accomplish:

- Detection: qualitative indication of the damage presence;
- Localization: information about probable location of the damage;
- Assessment: information about the damage size;
- Consequence: the actual safety of the damaged structure.

In this paper the Detection, Localization and Assessment of a damage with an Active/Passive SHM system has been investigated, piezoelectric transducers based in order to monitor the composite structures and it has also been explained the procedure for the validation system.

Guided wave technique

Observed for the first time by Horace Lamb in 1917, ultrasonic guided waves, or Lamb waves, are the base for a great number of new brands applications in inspection method [11,13,15-18,20]. This kind of micro-oscillations at very high frequency travels along the surface of the material in a non-dispersive way. Such specific property allows the perturbations to travel for long distances without loose too much energy, even inside materials with high attenuation ratio, as composites. Figure 3 shows the physical phenomenon of Lamb waves propagation on laminates and the principal modes of oscillation (symmetric and anti-symmetric) through the laminate thickness.

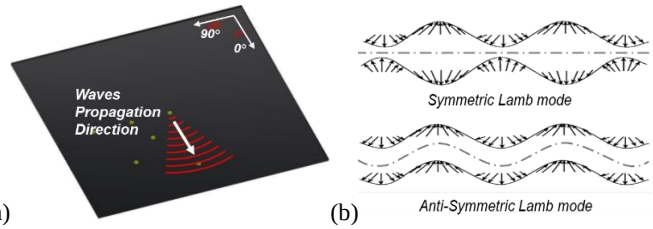

Figure 3: Representation of waves propagation direction on a laminate between two points (a) and Lamb waves modes (b).

The great sensitivity towards any kind of defect whether for metallic (as fatigue crack development, corrosion, bonding/debonding of joints, stress corrosion cracking or impact damage) or for composite materials (as impact, delamination, debonding for interface fiber intra-layers or matrix cracking) makes them suitable for inspection techniques. Indeed, when Lamb waves meet obstacles along their path, phenomena such as reflection, energy attenuation or scattering appear on the propagated signal.
Coupling the Lamb wave detection techniques with piezoelectric transducers is simple and efficient. An impulsive signal can be sent at high frequency by a piezo that works as an actuator and then it can be received by another piezo that acts as a sensor. A schematic representation of a monitoring system based on guided waves method coupled with piezoelectric transducers is shown in Figure 4.

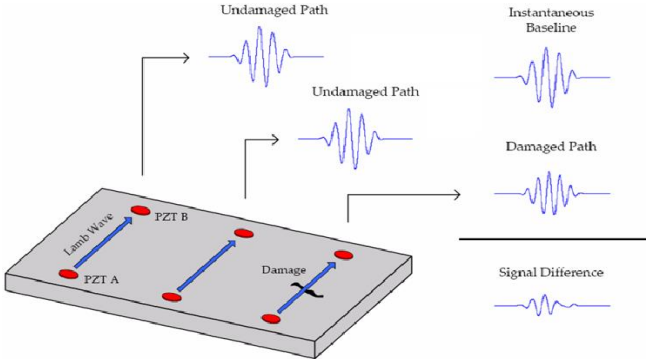

Figure 4: Schematic representation of a monitoring system based on guided waves method coupled with piezoelectric transducers.

The electrical Voltage signal imposed to the piezo actuator is converted by the inverse piezoelectricity into a strain signal, which travels along the structure. Thus, the piezo sensor converts the strain into a voltage signal by direct piezoelectricity. Hence, a comparison between clear path data and actual path data is performed in order to assess health status for the structure: the more the two signals are different the worse is the structure integrity. Thanks to a damage index specifically calculated, according to mm application involved, damage class and size characterization can be performed. If the sensors and actuators network is arranged in an appropriate configuration, as in Figure 5 for example, an algorithm for localization can be implemented, in order to correlate the wave distortion with the obstacle position. Guided waves technique allows to refer the actual acquisition to a general baseline, obtaining also the time at which a defect is generated. The excitation right frequency cannot be defined *a priori*, because it is a function of material properties, thickness and geometry of the component, so an initial tuning operation is needed.

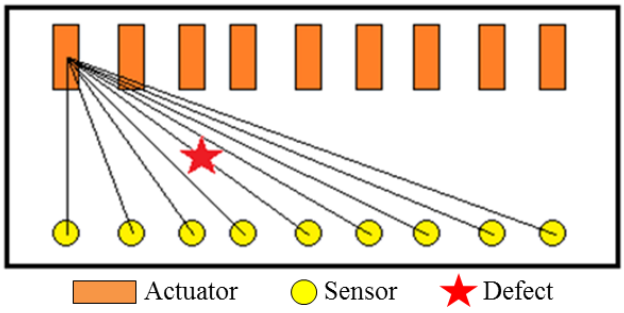

Figure 5: Example of a piezoelectric network for localization of a defect (star).

Materials

Composite samples

The composite material used for the case studies is an Epoxy resin reinforced with Carbon fiber T300 Twill 2x2, obtained by Prepreg lay-up and Vacuum-bag curing. The main mechanical properties of the composite material are reported in Table 2. Two kinds of samples have been obtained

from the laminates by Waterjet cut technique that avoids material thermo-degradation. The samples picture and the overall characteristics are reported in Figure 6 and Table 3.

Table 2: Mechanical properties of the composite material Carbon fiber/Epoxy.

Young Modulus [GPa]	58
Ultimate Tensile Strength [MPa]	570
Material Density [kg/m^3]	1460

Table 3: Overall characteristics of the composite samples.

Reinforcement	**Carbon fiber T300 Twill 2x2**	
Polymeric Matrix	**Epoxy Resin**	
Geometry	Beam	Plate
Dimensions [mm]	300x12	250x250
Overall thickness [mm]	1.0	4.6
Stacking Sequence	$[0°]_4$	$[0°]_{18}$
Thickness per layer [mm]	0.25	0.25
Productive Process	Prepreg hand lay-up, Water jet cut	Prepreg hand lay-up, Water jet cut

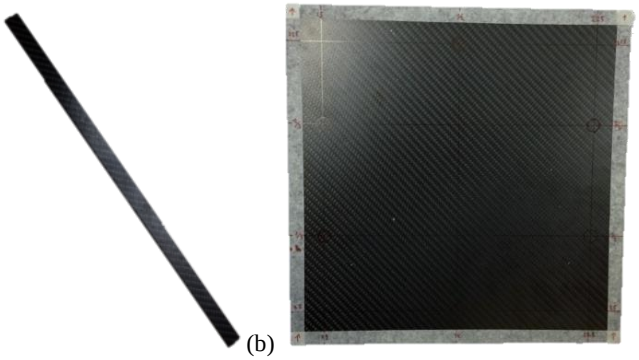

(a) (b)

Figure 6: Pictures of the composite samples: beam (a) and plate (b).

Piezoceramic Transducers

DuraAct piezoceramic transducers, supplied by Phisik Instrumente (PI) GmbH & Co. KG - Germany, have been selected because of their high versatility both for actuator and for sensor application. The main feature for this class of devices is the ability to support deformations without compromising the correct operations in transmitting and acquiring electrical signals. As results, DuraAct patches can be bonded to curved surfaces, differently from classic piezoceramics that break because of their excessive strain. Flexibility is provided by embedding the piezoelectric core inside two GRP layers, Figure 7 (a), that are then laminated in vacuum. Additionally, the coupling with the flexible material makes the piezoelectric core electrically insulated from the external environment. Furthermore, PI can provide customizable solutions as regards size, shape and thickness, according to the application requirements, as showed in Figure 7 (b).

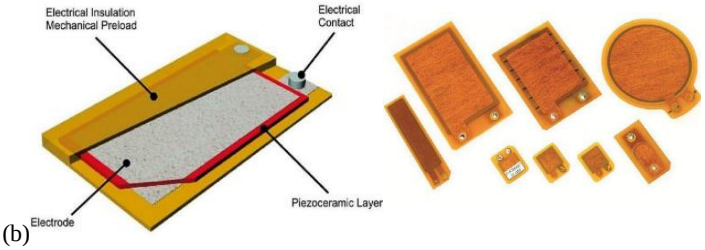

(a) (b)

Figure 7: Scheme of construction of a PI piezo transducer (a) and the PI commercial series of transducers (b) [21].

For the reported research activity, PI has customized two kinds of piezoelectric transducers with a specific request in dimensions and characteristics, as shown in Figure 8 and Table 4.

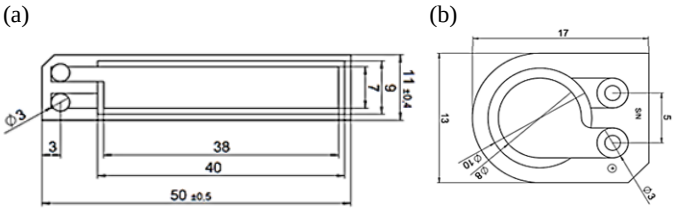

Figure 8: Dimensions of chosen PI piezo transducers [21].

Table 4: General characteristics of chosen PI piezo transducers.

Commercial name	**DuraAct P876-K015**	**DuraAct P876-K025**
Piezoceramic core material	PIC 255	PIC 255
Density [g/cm³]	7.8	7.8
Dimension of active plate [mm]	40 x 9 x 0.2	ϕ10 x 0.2
Flexible elastic external layers	Polyimide (Kapton)	Polyimide (Kapton)
Capacitance [nF]	20 ± 20%	20 ± 20%
Resonance frequency [kHz]	150	150
Curie temperature [°C]	350	350
Operating temperature [°C]	-40 to 150	-40 to 150
Mass for each transducer [g]	0.7512	0.2255

Test Equipment

Signal Generation/Acquisition

The system realized for SHM evaluation on a composite sample is shown in Figure 9. It is important to assure a high sample rate due to the propagation high frequency for the Lamb waves. Thus, to accomplish this task .it has been selected the National Instrument NI-6259 Multifunction I/O Device. kmA Multiplexer (MUX) TI-CD74HC4052 device has been used for the switching operation of the actuation-sensing of piezo transducers. The instruments main technical specifications are summarized in Table 5.

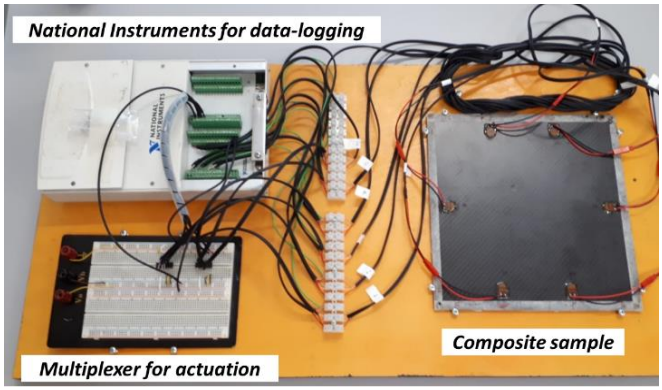

Figure 9: System realized for SHM evaluation on a composite sample.

Table 5: Technical specifications of Multifunction I/O Device (NI-6259) and Multiplexer - MUX (TI-CD74HC4052).

Multifunction I/O Device (NI-6259)		**Multiplexer - MUX (TI-CD74HC4052)**
Analog Output	**Analog Input**	**DC Supply**
4 channels	16 differential,	V_{CC} -0.5 to +7 V

	32 single handed	
Max. ±10 V	Max. ±10 V	V_{EE} +0.5 to -7 V
Resolution 16 bit	Resolution 16 bit	V_{CC}-V_{EE} -0.5 to +10.5 V
Sample Rate 2.86 Msamples/s	Sample Rate 1.00 Msamples/s	

The NI-6259 Multifunction I/O Device is controlled by a computer interface built in MATLAB environment. For the excitation signal, a sinusoidal burst is selected as resulted from the trials on the signal shape supported by piezo transducers. An impulse shape is given by the function shown in the Figure 10.

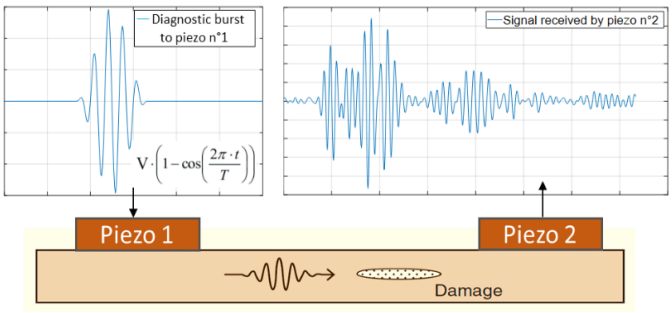

Figure 10: Schematic representation of voltage signal given to piezo 1 and obtained by piezo 2 as function of the structure health status.

The frequency of the diagnostic burst is controlled, and it is imposed at 40, 50, 75, 100 kHz, in order to evaluate the system response at different frequencies. The amplitude of exciting voltage as output from the NI-6259 module remains constant at 3.5 V, without modification caused by Multiplexer. The received voltage signal from the piezo sensors has been recorded by the NI-6259 as input and transferred to the MATLAB algorithm, which performs the data processing.

Damage Generation

The Instron CEAST 9350 for drop-dart impact testing, shown in Figure 11, has been used in order to obtain repeatable damages and to collect the load during the dynamic test of the composite plate.

a)  b) 

Figure 11: Instron CEAST 9350 for drop-dart impact testing (a) and a detail of composite plate ready for the dynamic test (b).

C-Scan Analysis

To evaluate the entity of the damage generated with the drop-dart impact machine, a C-Scan Analysis has been conducted on composite plate using an Olympus OmniScan SX, a device based on phased array technique and equipped with a near-wall probe of 64 piezo elements. The experimental setup is shown in Figure 12.

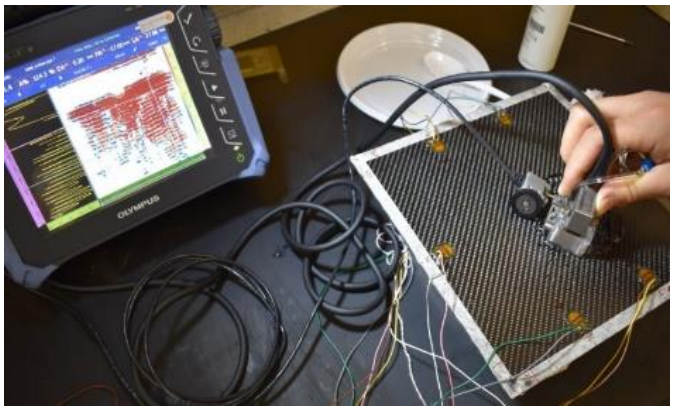

Figure 12: Experimental setup for the C-Scan investigation with Olympus OmniScan SX device.

System Validation

In the application implemented, vibrations generated by piezoelectric actuator are collected through a measurement system made up by piezoelectric sensors. To complete this task, both aspects, transmission and receiving of signals, must be well known, with a deep knowledge about:

- Coupling effect between transducers and host structure;
- Shape of signal supported for propagation;
- Effectiveness of the signal transmission for various exciting frequencies;
- Wave propagation on the composite material surface.

To gather knowledge about these parameters and to obtain a tuning for the specific application of damage detection over a beam in composite material, some experimental tests have been conducted.

Piezo-Structure Coupling effect

When an external electrical signal, with low amplitude and high frequency, is used as input for a piezoelectric patch bonded to a host structure, the micro displacement induced by the piezo contraction, Figure 13 (a), travels inside the material as a wave. If a second transducer is coupled to the same structure in a different position without any electrical excitation, a signal as output can be detected. The received signal amplitude is a function of the bonding quality between the piezo patches and the host structure.

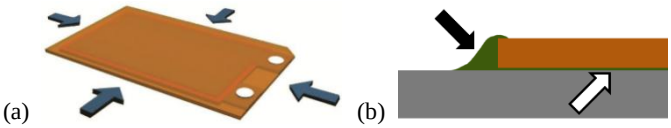

Figure 13: Strain due to inverse piezoelectricity from an applied electric voltage (a) and the PI recommended bonding specifications for the coupling (b) [21].

For the beam sample, two rectangular DuraAct P876-K015 have been coupled to the composite in order to evaluate the coupling influence to the signal transmission. Two different bonding techniques have been tested, as shown in Figure 14: a special flash tape and epoxy resin, as recommended by PI technical datasheet, Figure 13 (b) [21].

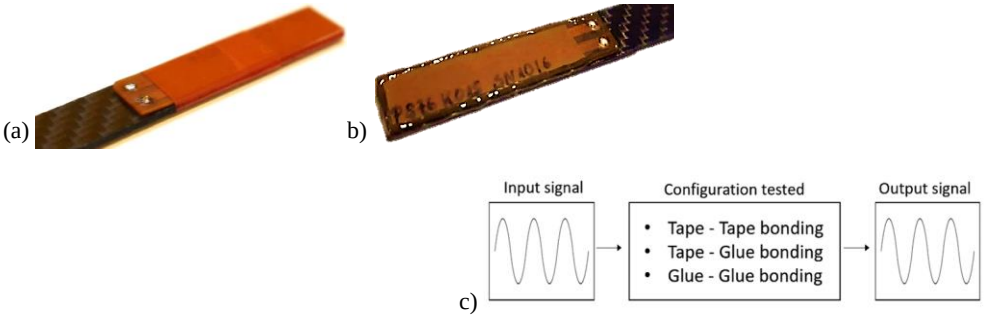

Figure 14: Bonding of rectangular piezo patch to the composite beam with special flash tape (a) and epoxy resin, as recommended by PI (b). Coupling effect study with different bonding configuration (c).

For the plate sample, six circular DuraAct P876-K025 have been coupled to the composite with epoxy resin, as recommended by PI. The choice to introduce these piezoelectric patches geometry is the circular wave propagation, in order to have the same stimulation between the couples of piezo not positioned face to face.

Figure 15: Bonding of circular piezo patch to the composite plate with epoxy resin, as recommended by PI (b).

The piezo transducers on the beam have been positioned on the opposite edges, as in Figure 16: the piezo n°1 is the actuator and it gives the exciting signal at the root, the piezo n°2 is the sensor and gets the propagated signal at tip, so that it is called “pitch-catch”.

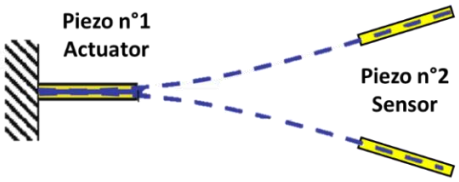

Figure 16: Experimental scheme for the frequency effect evaluation on the composite beam.

The excitation signal is a sinusoidal wave of amplitude ±12 V and frequency from 2 Hz to 2 MHz. The coupling has been tested in configuration tape-tape, tape-glue and glue-glue for the actuator and sensors. The different couplings effectiveness was evaluated with an oscilloscope and the wave analysis highlighted the following:

- For tape-tape configuration, at low frequency the signal transmission is inefficient both for amplitude and for frequency, at higher frequency the sensed amplitude does not change, while the sensed frequency can be clearly detected.
- For tape-glue configuration, at low frequency the signal transmission remains inefficient, at higher frequency the sensed amplitude can be clearly detected without ambiguity with instrumental noise and the peak-to-peak voltage values change according to the frequency with a non-linear behavior.
- For glue-glue configuration, at low frequency, the signal amplitude is well detected by the sensor and it is higher than the tape tests. This improvement is probably related with the better bonding quality that allows a proper wave transmission between the piezoelectric patches and the host structure.

Figure 17 shows the behavior of piezo n°2 (tip) at different frequencies. The Output Voltage Amplitude reach the maximum value at 2 kHz for the glue-glue bonding onto the composite beam.

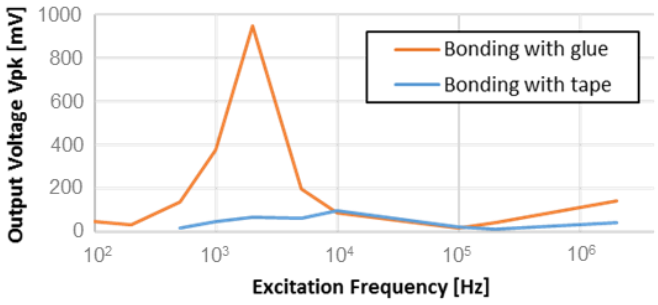

Figure 17: Output Voltage-Excitation vs. Frequency excitation for the glue-glue and tape-tape bonding of piezo n°2 (tip) onto the composite beam.

Shape of signal supported

When a sensor receives a signal transmitted by an actuator, some distortion with regard to the external input can be detected. For this reason, the distortion typology investigation has an important role in order to distinguish if it is caused by the natural propagation inside the material or if it is due to a failure in transmission. As a matter of fact, sinusoidal, square and triangular wave shapes have been sent to the piezo actuator with a constant amplitude of ±12 V, in order to characterize the effective reproducibility of the wave shape. For each wave shape, different excitation frequencies have been imposed, in order to evaluate the transmission behavior (Table 6).

Table 6: Analysis of wave shape transmission from piezo actuator to piezo sensors.

Exciting Frequency	Sinusoidal wave	Square wave	Triangular wave
17 Hz	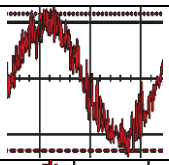	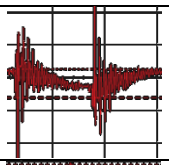	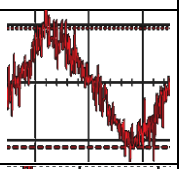
500 Hz	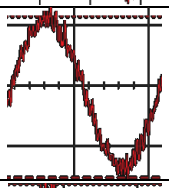	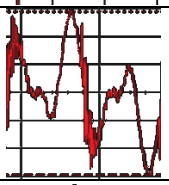	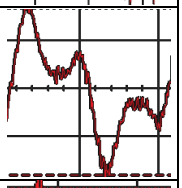
10 kHz	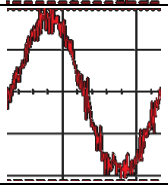	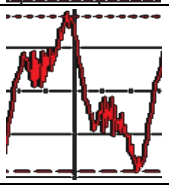	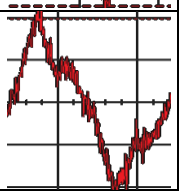

The sinusoidal wave is the only input shape that is perfectly transmitted and received at any frequencies. On the contrary, triangular wave is subjected to distortion at low frequencies and it becomes acceptable just at the higher ones, while the square wave is not received well neither at high nor at low excitation.

The problem in transmitting for impulsive signal, such as the square and the triangular waves, is probably due to the piezo inability to send irregular signals. This result is very important because it underlines the fact that only a piezoelectric system constituted by actuators and sensors can transmit and receive sinusoidal signals.

Frequency effect

In order to quantify the influence of the exciting frequency to the sensed signal, one piezo actuator has been glued at the composite beam root, one piezo sensor at the tip and one piezo sensor at the root of opposite side actuator. Figure 18 shows a schematic representation of the beam sample arrangement.

Figure 18: Experimental scheme for the frequency effect evaluation on the composite beam.

The frequency of the sinusoidal signal changed in a range from 1 Hz to 1 MHz. The response most significant results for tip and root have been reported, in order to have an Output Voltage values overview in different zones of the composite beam.
At frequency of 1 Hz, the signal sensed at the tip cannot be distinguished because of noise interference; at the root, the acquisition is sufficiently good as shown in

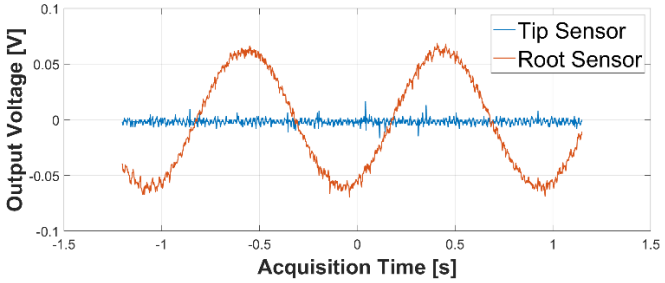

Figure 19.

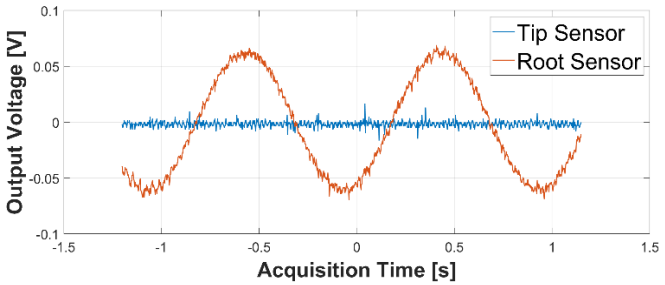

Figure 19: Output Voltage vs. Time for the piezo sensors at root and tip at the exciting frequency of 1 Hz.

At 100 Hz the sensed frequency is well reproduced, and the output voltage is clearly distinguished from noise, as shown in Figure 20.

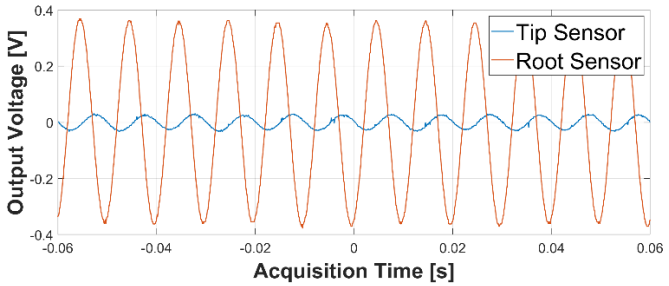

Figure 20: Output Voltage vs. Time for the piezo sensors at root and tip at the exciting frequency of 100 Hz.

It is important to note that the Output Voltage values for the piezo sensor at the root are generally higher than the piezo sensor at the tip. This result is probably related to the energy dissipation at higher distances from the exciting place. In terms of acoustic propagation, if the frequencies increase, the waves travel far away from the source. Hence, the need to impose a high frequency for sending the input signal in a SHM system. An overview of sensed frequency is shown in **Errore. L'origine riferimento non è stata trovata.**, with the Output Voltage Amplitude for root and tip sensors.

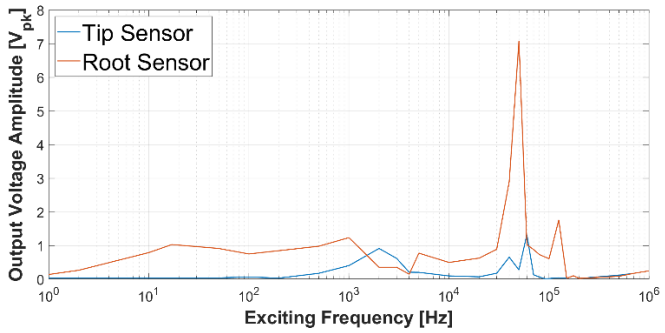

Figure 21: Output Voltage Amplitude vs. Frequency for piezo sensors at root and tip in the range of frequency from 1 Hz to 1 MHz.

In conclusion, the best frequency for the strain signal transmission, in this experimental configuration, is 50 kHz. This value will be used for the validation of the SHM system. Figure 22 shows the response for root and tip sensors, at the chosen excitation frequency of 50 kHz.

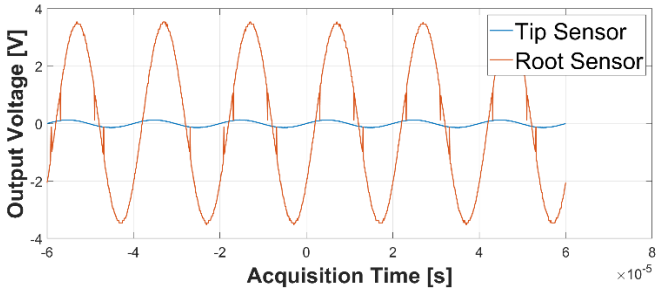

Figure 22: Output Voltage vs. Time for the piezo sensors at root and tip at the exciting frequency of 50 kHz.

Data Processing

Damage Detection

The Reconstruction Algorithm for Probabilistic Inspection of Defects (RAPID) [15] has been used for the defect detection. A piezoelectric patches network is bonded to a host structure. Each sensor works as an actuator or a sensor. One after the other, each piezoelectric transducer sends a signal that spreads on the monitored structure surface. The signals for each couple of actuator-sensor are gathered for each possible combination.

These acquired data are processed in order to compute a damage index that considers the structure health. The higher is the value calculated, the worse will be the structure health status. The damage index is evaluated by comparing actual signal with a reference one, collected from the specific couple i-j.

$$A_{ij} = 1 - \frac{C_{XY}}{\sigma_X \sigma_Y} \qquad (1)$$

$$C_{XY} = \sum_{k=1}^{K} (X_k - \mu_X)(Y_k - \mu_Y) \qquad (2)$$

$$\sigma_X \sigma_Y = \sqrt{\sum_{k=1}^{K} (X_k - \mu_X)^2} \sqrt{\sum_{k=1}^{K} (Y_k - \mu_Y)^2} \qquad (3)$$

Where:

- A is the damage index
- X is the set of Voltage data for reference signal
- Y is the set of Voltage data for the actual signal acquired
- μ is the Voltage average
- C is the covariance
- σ is the standard deviation

It is important to note that RAPID algorithm is a method essentially based on comparison between two data sets. For the calculation of the damage index A, it is not important how the wave travels inside the material, or how the interactions with boundary condition change the data magnitude. The only requested requirement is to reproduce for each acquisition the exact condition in which the baseline data have been recorded. In case of different test conditions, a proper calibration of the system must be carried on, evaluating the damage index at different temperatures, relative humidity and stress/strain boundaries.

Damage Localization

The localization of a defect can be realized only inside the region delimited by the transducers network, so a damage map must be generated. This network discretizes the covered area in ellipses, in which the piezo patches are the focal points. The ellipse size is related to the β parameter: in Figure 23 the red ellipse has a β value higher than the yellow one.

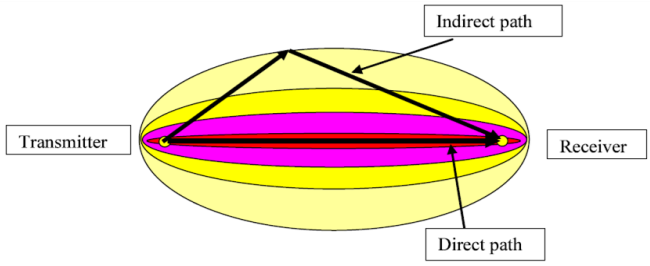

Figure 23: Elliptical map of interaction for piezo couple of actuator-sensor [15].

To determine the defect distribution probability, an index P for the specific couple i-j is calculated for each point (x,y) of the network.

$$R_{ij}(x,y) = \begin{cases} RD_{ij}(x,y) & when\ RD_{ij}(x,y) < \beta \\ \beta & when\ RD_{ij}(x,y) \geq \beta \end{cases} \qquad (5)$$

$$P(x,y) = \sum_{i=1}^{N-1} \sum_{j=i+1}^{N} A_{ij} \left[\frac{\beta - R_{ij}(x,y)}{\beta - 1} \right] \qquad (4)$$

$$RD_{ij}(x,y) = \frac{\sqrt{(x-x_i)^2 + (y-y_i)^2} + \sqrt{(x-x_j)^2 + (y-y_j)^2}}{\sqrt{(x_j-x_i)^2 + (y_j-y_i)^2}} \qquad (6)$$

Where:

- P(x,y) is the defect distribution probability at point (x,y)

- N is the total number of piezo patches on the structure
- β is a parameter which controls the size of the ellipses
- $R_{ij}(x,y)$ relates to the inclusion of point (x,y) in the ellipse
- $RD_{ij}(x,y)$ is the ratio of the sum of distances of point (x,y) to the focal points to the distance between focal points

The position of the point (x,y) relative to the i-j ellipse has influence on the damage index, calculated in this point from the analysis of the data sets. The possible cases are the following:

- Point (x,y) is along the direct path, $RD_{ij}=1$, the damage index is considered entirely on the damage map.
- Point (x,y) is outside the ellipse, RD_{ij} is higher than β, the contribution to the damage index is locally null.
- Point (x,y) is inside the ellipse along an indirect direct path, RD_{ij} is lower than β, the contribution to the damage index is linearly decreasing from the direct path to the edge of the ellipse.
- Point (x,y) is included in more than one ellipse, the damage index values of the relative piezo couples will be summed, and a final higher damage index is calculated.

Virtual application of RAPID algorithm

In order to test the algorithm effectiveness, a virtual application in MATLAB (Appendix A) has been implemented. A six piezoelectric patches network are virtually arranged over a rectangular area with dimensions, as shown in Figure 24.

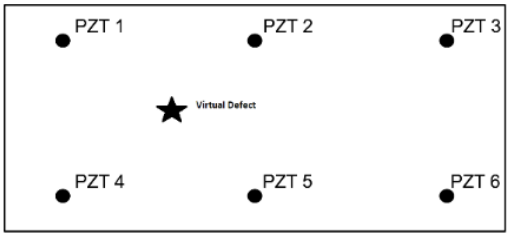

Figure 24: Network of six piezoelectric patches arranged on a virtual plate.

The area covered by each data transmission between two couples of transducers depends on the value of β. Three different configurations with β equal to 1.01, 1.05 and 1.1 are shown in Figure 25.

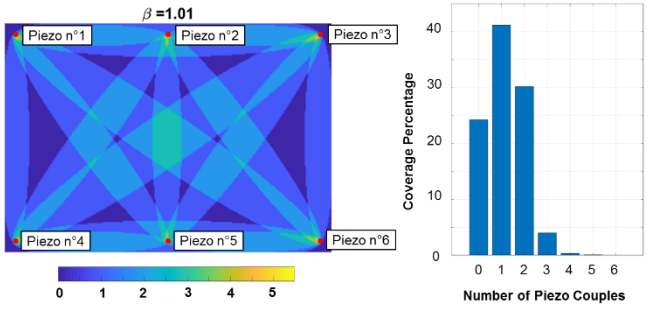

a)

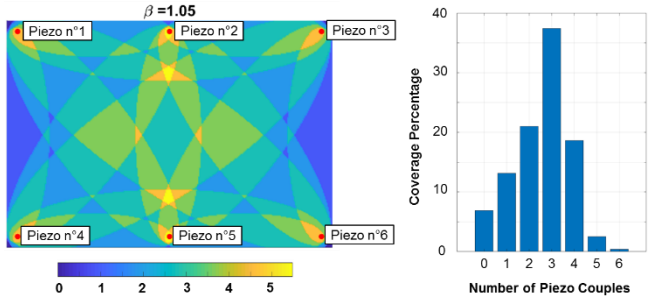

b)

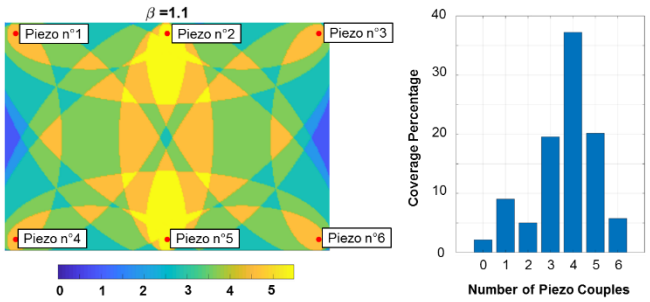

c)

Figure 25: Covered area for the piezo couples at values of β equal to 1.01 (a), 1.05 (b) and 1.1 (c).

The increasing of the influence area for each couple generates a larger area covered by the damage inspection. On the other hand, the accuracy for damage localization decreases, because the damage index is spread on an area instead to be localized on a single point. The β value of 1.05 is the trade-off between accuracy and a large covered area, as reported in the literature [15].

To verify the algorithm effectiveness, an artificial distortion of the virtual data has been generated and used as input for the MATLAB implemented script. In order to simulate the presence of defects between piezoelectric transducers number 1 and 5, and between number 2 and 4, different sets of data are imposed as reference and test signals. Figure 26 shows the distortion relative to a reference baseline for the virtual acquisition with piezo 1 as actuator. The artificial distortion between the reference and the actual signal generates values different from zero, for A15, A24, A51, A42, equal to 1.37. As a result, the sum of damage indices for a damage map generation that is four times A15, equal to 5.48. Local damage index values are employed to generate the defect map. Figure 27 shows the highest probability of defect presence in correspondence of modified data sets.

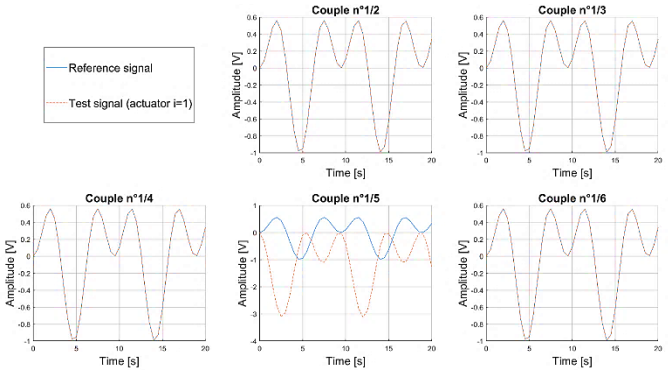

Figure 26: Artificial distortion of the data set for virtual acquisition of piezo 1 as actuator and piezo 2,3,4,5,6 as receivers.

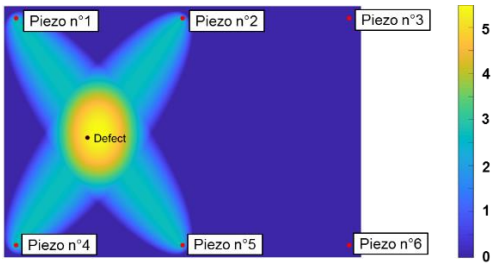

Figure 27: Damage map with high probability of defect presence between piezo couples 1-5 and 2-4.

Covered area effect

Thanks to the radial propagation, different configurations for the transducers network can be arranged. An investigation has been carried out with the aim to identify the best disposition in terms of covered area for the defect detection when six devices are employed. The final comparison between "hourglass" and circular configurations for sensor positioning is reported in Figure 28.
In comparison with the "hourglass" positioning, the circular disposition of the six piezo has a smaller global coverage area, but the surface inspected by at least three piezo couples is greater than that is inspected by only one piezo couple. The final disposition of the piezoelectric transducers on the composite plate is shown in Figure 29.

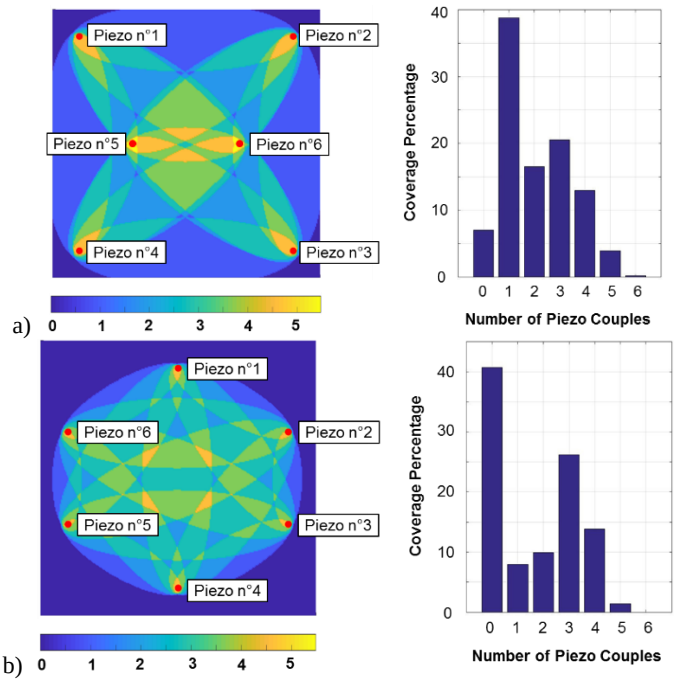

Figure 28: Covered area related to "hourglass" (a) and circular (b) configurations for sensor positioning on the composite plate.

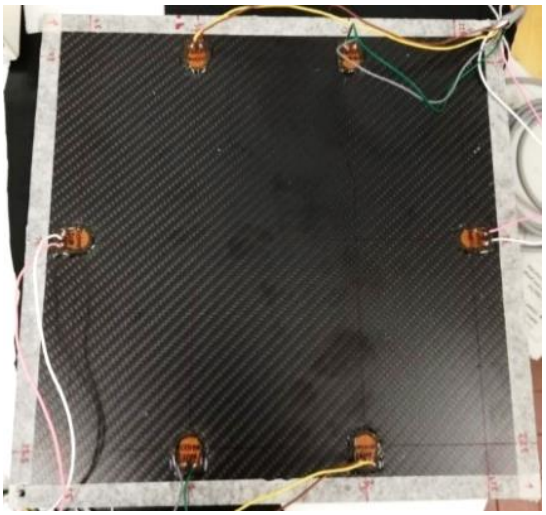

Figure 29: Final arrangement of piezo transducers on the composite plate.

Waves propagation over the composite

The orthotropic properties of the composite material do not affect only the laminate mechanical behavior. In Figure 30 is reported the Output Voltage maximum value as function of Input Voltage and Exciting Frequency for the wave propagation on the fibers (piezo couple 2-6) and across the fibers on the plate (piezo couple 2-5), changing piezo couples. A signal significative peak has been found for propagation on fibers at 40 kHz.

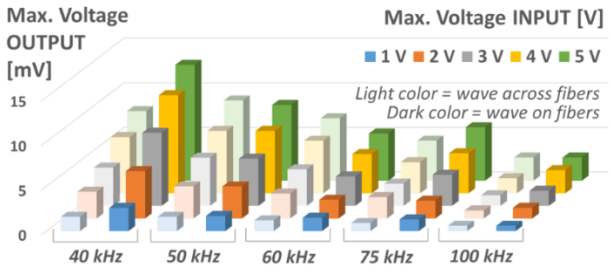

Figure 30: Maximum value of Output Voltage as function of Input Voltage and Exciting Frequency for the wave propagation on the fibers and across the fibers.

Experimental procedure

Firstly, a baseline acquisition for the healthy structure without any damage has been effectuated either for beam or for plate. After that, an external defect has been generated on the sample surface and a second data acquisition has been recorded. The defect presence that induces a distortion in the guided waves propagation, has been demonstrated, through the comparison between the two data sets. Figure 3131 shows a schematic representation of the steps required for experimental investigation for beam and plate.

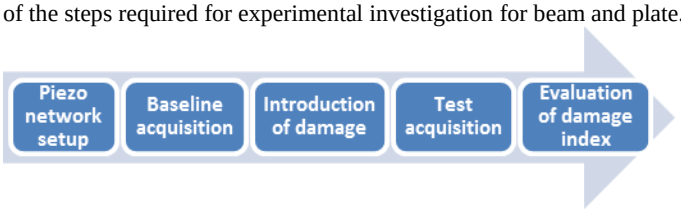

Figure 31: Schematic representation of the experimental procedure.

Damage Detection and Assessment

Firstly, a comparison between two measurements without any induced defects has been conducted on the beam sample, in order to assess the test system repeatability. The measurement chain has been schematized in Figure 32. Although some external effects can slightly change the signal acquisition during the two tests, it is expected a damage index near to zero for the damage map. In Figure 33 a, it is plotted the comparison between two consecutive measures without induced defect. The two signals, as predicted, are quite similar, and it is confirmed also by the low damage index in the damage map, reported in Figure 33 b, equal to 0.00035.

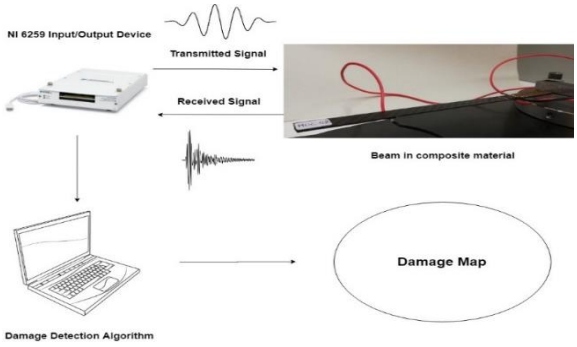

Figure 32: Measurement chain for the Detection and Assessment of damages.

a)

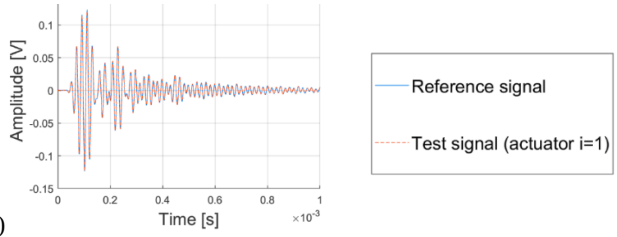

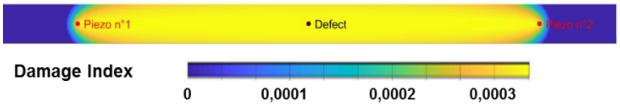

b)

Figure 33: Comparison between two consecutive measures without defect (a) and the related damage index on the damage map (b).

Subsequently, a real damage is generated on the beam. A pointer and a hammer have induced three consecutive impacts in the same point on the structure surface, as shown in Figure 34 (a). For each damage, an inspection has been carried out using the RAPID algorithm and then the results for damage index have been calculated. Because of the defect growth, an increasing value for the damage index predicted has been observed, through a non-linear behavior, as shown in Figure 34 (b).

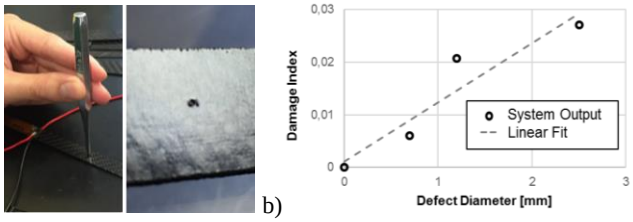

a) b)

Figure 34: Damage generation on the beam (a) and Damage index correlation with the defect size (b).

In Figure 35 is reported the comparison between recorded signals, with a defect increasing size while in Figure 36 the damage maps shows the good evaluation of the defect size by the SHM system.

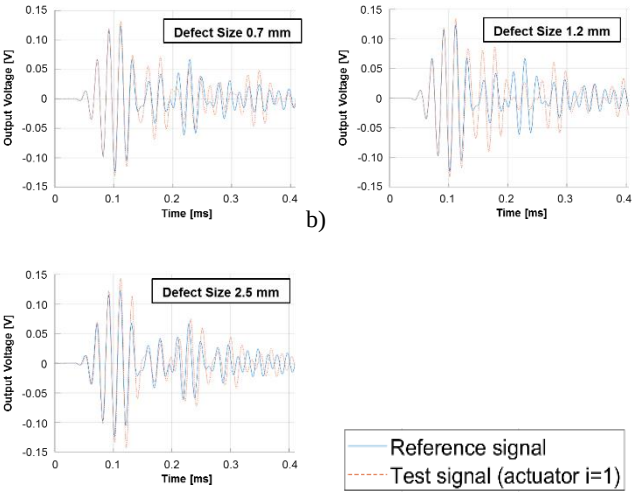

a) b) c)

Figure 35: Example of acquired data, in blue the reference, in red the test acquisition for each stage of damage.

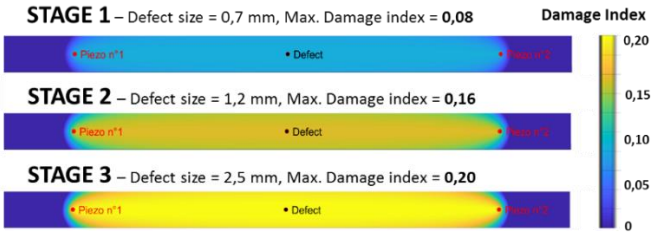

Figure 36: Maximum Damage index and Damage map for the three stages.

The experimental setup for SHM evaluation on a composite structure have been achieved, it is possible to highlight that:

- Interferences due to external noise are low compared with the distortion generated by the presence of a real defect;
- Damage index is proportional to defect size;
- Localization can be performed with at least three sensors in order to obtain triangulation of the signals.

Damage Detection, Assessment and Localization

An experimental test with the plate in composite material has been set. The main difference with the beam case study is the chance to engage the defect detection through a plurality of transducers. This feature allows adding the damage localization to the basic feature of detection. Four impact stages by different impactor velocity have been conducted, as in Table 7, resulting in different Load curves (Figure 37). The first two impacts were made on piezo side of the plate, the last two on the other side, in order to produce different damages and understand the SHM system effectiveness on both sides. After each impact the visual and the C-SCAN inspections have been carried out; the pictures are reported in Figure 38 and Figure 39.

A final analysis has been carried out in order to characterize the defect size using the SHM method. As previously done for the beam, a maximum damage index is calculated for different defect sizes.

Table 7: Experimental specifications for impact test of the composite plate.

	Stage			
	1	**2**	**3**	**4**
Impact Velocity [m/s]	1.55	1.75	1.55	2.15
Impact Energy [J]	5	7	5	12
Impacted Plate Side	Top	Top	Bottom	Bottom
Damaged Plate Side	Top	Top	Top	Top
Damage	Imprint	Imprint	Crack	Crack

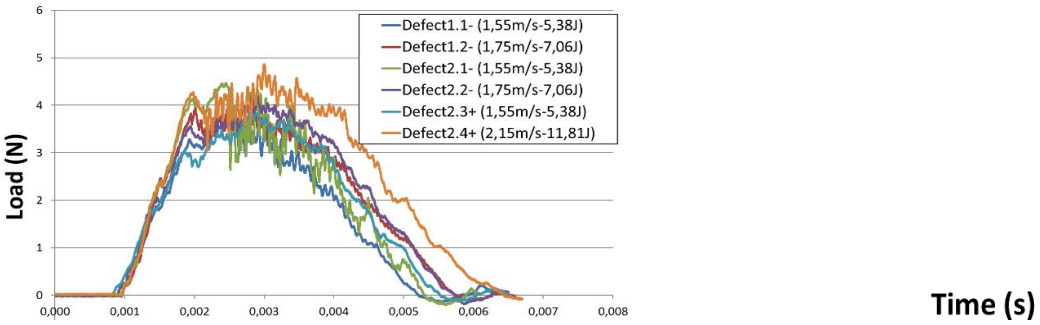

Figure 37: Load-Time impact curves for the four stages of damage.

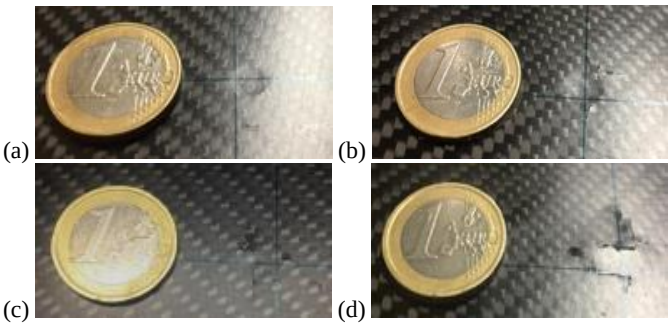

Figure 38: Visual inspection of the four stages on the composite beam.

To evaluate the influence of the boundary conditions, two different configurations has been tested for the plate: appended “free-free” and clamped with steel plates to an anti-vibrating table, as shown in Figure 40.

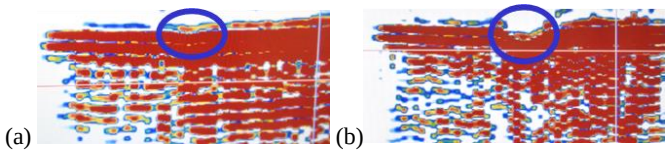

(c) (d)

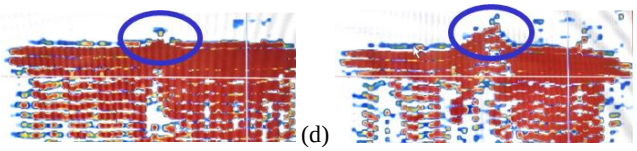

Figure 39: C-Scan inspection of the four stages on the composite beam.

a) b)

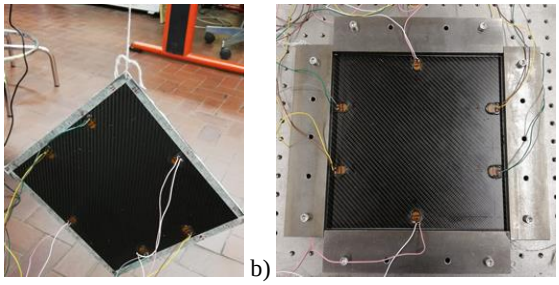

Figure 40: Appended (a) and clamped (b) configuration for the plate testing.

Figure 41 shows the data baseline sets for the piezo 1-2 couple, at the 50 kHz exciting input. To cut external noise, data were filtered by low-pass filter at exciting frequency.

Despite the structural conditions are the same, different data sets have been acquired. Consequently, each configuration needs its proper baseline acquisition. Then, the comparison between reference and actual signals for each defect has been analyzed. The actuation signal is a sinusoidal burst. For the right excitation signal definition, the test frequency changed in the range 100 Hz to 125 kHz. For low frequency of 100 Hz, a low amplitude mechanical vibration is induced and the sinusoidal signal transmitted cannot be distinguished, as plotted in Figure 42.

a)

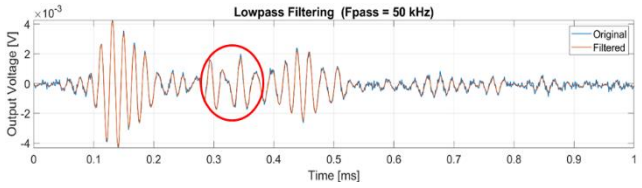

b)

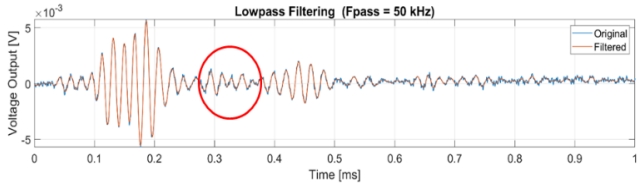

Figure 41: Low-pass filter at exciting frequency applied to the baseline data sets for the appended (a) and clamped (b) configurations.

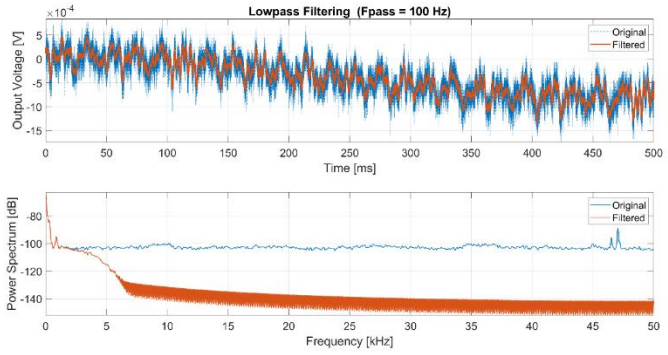

Figure 42: Low-pass filter at exciting frequency applied to an example of the acquisition data sets at 100 Hz.

At the higher frequency of 5 kHz, as shown in

Figure 43, the sinusoidal wave is distinguishable, due to the mechanical vibration disappearance. The power spectrum shows a peak at 5 kHz.

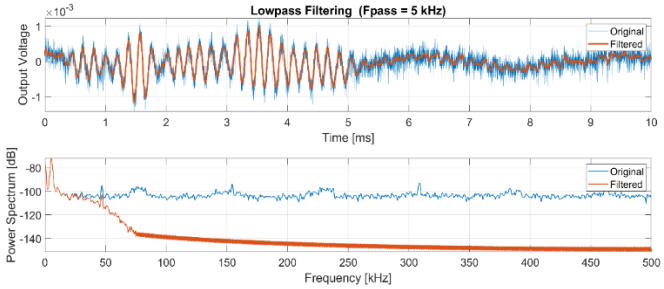

Figure 43: Low-pass filter at exciting frequency applied to an example of the acquisition data sets at 5 kHz.

Only the data recorded at higher frequencies (50-125 kHz) have been considered for SHM purpose, in order to overcome the structure mechanical vibrations. An example of data set acquired for all piezo couples with the piezo actuator n°6 is reported in Figure 44.

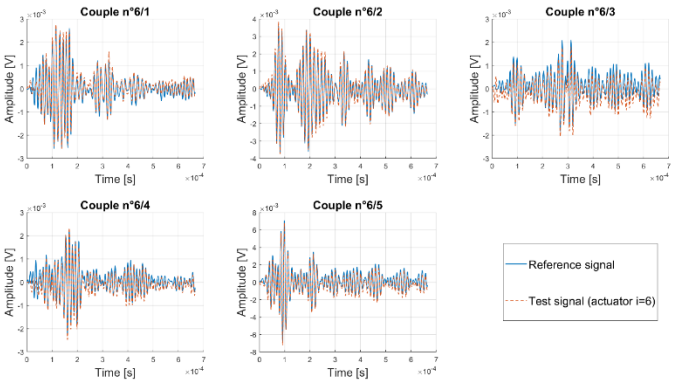

Figure 44: Example of filtered data set acquired for all piezo couples with the piezo actuator n°6.

The damage maps for the defect assessment and localization at the 60 kHz exciting frequency for the damage stages are shown in Figure 45 and Figure 46, respectively for the appended and clamped plate. The Figure 47 shows the real position of the defect on the composite plate. In the figures, the Defect 1 is a previous trial damage while the Defect 2 is the damage discussed in this paper.

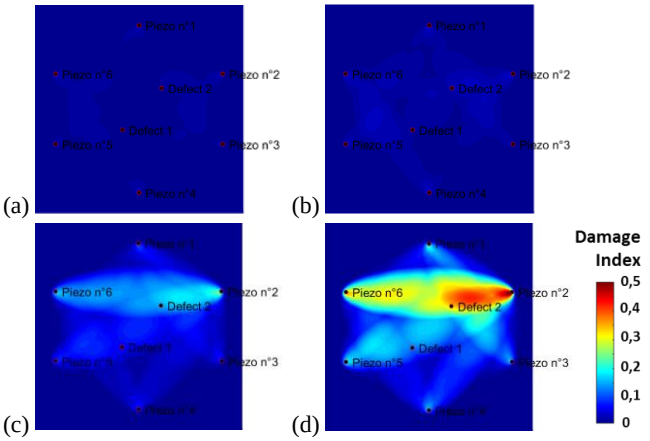

Figure 45: Damage map of the four stage of defect for the appended plate.

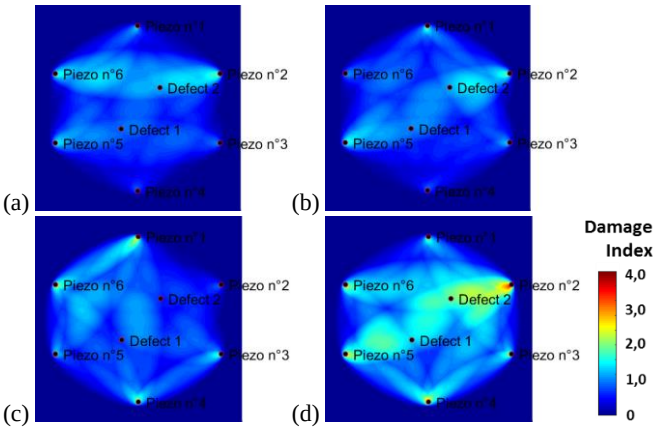

Figure 46: Damage map of the four stage of defect for the clamped plate.

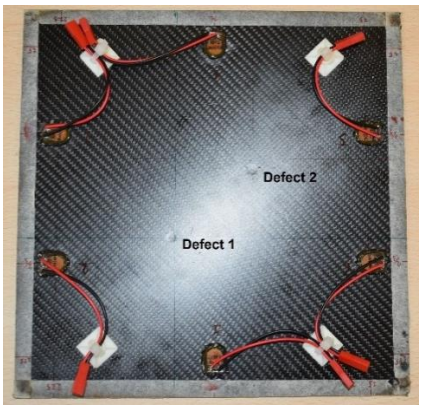

Figure 47: Position of the defect 1 and defect 2 on the composite plate.

Results

Owing to the experimental test for a SHM evaluation on a plate in composite material, some results can be highlighted:

- Different behavior in baseline acquisition is observed with two different boundary condition for the constraints: “free-free” and clamped over all the edge;
- Interferences due to external noise are comparable with distortion generated by the presence of a real defect;
- Detection of a defect is well realized only with high frequency, where mechanical vibrations are completely dissipated;
- Localization of the defect inside the piezoelectric transducers network is reliable with the real position of artificial damage;
- Damage index is proportional to defect size;
- The system response is better if the damage is placed on the same surface of the piezo network.
- The boundaries generally increase the damage index values.

Conclusions

Nowadays, the massive use of composite materials for the innovative components design requires new methods for the structural integrity inspection. The aim of this work is the experimental investigation on piezoelectric transducers for a composite structural health monitoring. An evaluation about coupling quality has been conducted, the glued configuration has shown the best reconstruction of the sinusoidal signal, sent by a piezo actuator and received by a piezo sensor, both in output voltage and in frequency. The frequency study highlighted the best transmission at 50 kHz. Thanks to all the information gathered during the validation tests, two Structural Health Monitoring case studies on composite structures have been performed. The composite beam case study with two piezo on the opposite tips allowed the comparison between a reference signal for the structure in healthy condition and after a defect the generation. Thanks to the calculation of a damage index, the defect detection and the assessment have been carried out. In addition, increasing the defect diameter, the damage index has shown a proportional growth. The composite plate case study with six piezo at the edges allowed to maximize the piezo sensing covered area. A drop-dart impact test bench has realized four stages of damage at increasing energy, in order to evaluate the SHM response. The detection, assessment and localization of the damage have been carried out in two conditions, appended and clamped at the sides. The knowledge gained with experimental investigation of piezoelectric transducers for structural health monitoring makes possible further investigations in terms of research and industrial development.

References

1. Messana, A., Sisca, L., Ferraris, A., Airale, A.G., de Carvalho Pinheiro, H., Sanfilippo, P., and Carello, M., "From Design to Manufacture of a Carbon Fiber Monocoque for a Three-Wheeler Vehicle Prototype," *Materials* 12(3):332, 2019, doi:10.3390/ma12030332.
2. Carello, M., and Airale, A.G., "Composite Suspension Arm Optimization for the City Vehicle XAM 2.0," *Design and Computation of Modern Engineering Materials* 54:257-272, 2014, doi:10.1007/978-3-319-07383-5_18.
3. Xu, S., Ferraris, A., Airale, A.G., and Carello, M., "Elasto-kinematics design of an innovative composite material suspension system," *Mechanical Sciences* 8(1):11–22, 2017, doi:10.5194/ms-8-11-2017.
4. Fasana, A., Ferraris, A., Airale, A.G., Berti Polato, D., and Carello, M., "Oberst and aging tests of damped CFRP materials: New fitting procedure and experimental results," *Composites Part B: Engineering* 148:104-113, 2018, doi:10.1016/j.compositesb.2018.04.046.
5. Fasana, A., Ferraris, A., Berti Polato, D., Airale, A.G., and Carello, M., "Composite and Damping Materials Characterization with an Application to a Car Door," *Advances in Italian Mechanism Science* 68:174-184, 2019, ISBN:978-3-030-03319-4 978-3-030-03320-0.
6. Fasana, A., Ferraris, A., Airale, A.G., Berti Polato, D., and Carello, M., "Experimental Characterization of Damped CFRP Materials with an Application to a Lightweight Car Door," Shock and Vibration 2017:1-9, 2017, doi:10.1155/2017/7129058.
7. Fasana, A., Carello, M., Ferraris, A., Airale, A., and Berti Polato, D., "NVH Analysis of Automotive Components: A Carbon Fiber Suspension System Case," *Advances in Italian Mechanism Science* 47:345-354, 2017, doi:10.1007/978-3-319-48375-7_37.
8. Ferraris, A., Messana, A., Sisca, L., Santoro, F., Airale, A.G., and Carello, M., "Statistical Energy Analysis SEA: A Correlation Between Virtual and Experimental Results," *Advances in Italian Mechanism Science* 68:211-220, 2019, doi:10.1007/978-3-030-03320-0_23.
9. Virgillito, E., Airale, A.G., Ferraris, A., Sisca, L., and Carello, M., "Specific Energy Absorption Evaluation on GFRP Laminate Plate by Optical, Thermographic and Tomographic Analysis," *Experimental Techniques* 43(1):15-24, 2019, doi:10.1007/s40799-018-0257-y.
10. Balageas, D., Fritzen, C.-P., and Güemes, A., "Structural health monitoring," 2006, ISBN:9780470612071.
11. An, Y.-K., Kim, M.K., and Sohn, H., "Piezoelectric Transducers for Assessing and Monitoring Civil Infrastructures," *Sensor Technologies for Civil Infrastructures* 86–120, 2014, doi:10.1533/9780857099136.86.
12. Rytter, A., "Vibrational Based Inspection of Civil Engineering Structures," *Fracture and Dynamics* R9314(44), 1993.
13. Ihn, J.-B., and Chang, F.-K., "Detection and Monitoring of Hidden Fatigue Crack Growth Using a Built-in Piezoelectric Sensor/Actuator Network: I. Diagnostics," *Smart Materials and Structures* 13(3):609–20, 2004, doi:10.1088/0964-1726/13/3/020.
14. Zagrai, A.N., and Giurgiutiu, V., "Electro-Mechanical Impedance Method for Crack Detection in Thin Plates," *Journal of Intelligent Material Systems and Structures* 12(10):709–18, 2001, doi:10.1177/104538901320560355.
15. Zhao, X., Gao, H., Zhang, G., Ayhan, B., Yan, F., Chiman, K., and Rose, J.L., "Active Health Monitoring of an Aircraft Wing with Embedded Piezoelectric Sensor/Actuator Network: I. Defect Detection, Localization and Growth Monitoring," *Smart Materials and Structures* 16(4):1208–17, 2007, doi:10.1088/0964-1726/16/4/032.
16. Bartelds, G., "Aircraft Structural Health Monitoring, Prospects for Smart Solutions from a European Viewpoint," *Journal of Intelligent Material Systems and Structures* 9(11):906–10, 1998, doi:10.1177/1045389X9800901106.
17. Cai, J., Lei, Q., Shenfang, Y., Lihua, S., PeiPei, L., and Dong L., "Structural Health Monitoring for Composite Materials," *Composites and Their Applications* 2012, doi:10.5772/48215.
18. Di Sante, R., "Fibre Optic Sensors for Structural Health Monitoring of Aircraft Composite Structures: Recent Advances and Applications," *Sensors* 15(8):18666–713, 2015, doi:10.3390/s150818666.
19. Lin, M., and Fu-Kuo, C., "Composite Structures with Built-in Diagnostics," *Materials Today* 2(2):18-22, 1999, doi:10.1016/S1369-7021(99)80007-8.
20. Lin, M., Kumar, A., Qing, X., Beard, S.J., Russell, S.S., Walker, J.L., and Delay, T.K, "Monitoring the Integrity of Filament-Wound Structures Using Built-in Sensor Networks," *Proceedings of the SPIE* 5054:222-229, 2003, doi:10.1117/12.483877.
21. Physik Instrumente (PI) GmbH & Co. KG, Piezoelectric Actuators catalogue and datasheets (www.piceramic.com).

Contact Information

Massimiliana Carello:
Politecnico di Torino – Department of Mechanical and Aerospace Engineering
C.so Duca degli Abruzzi, 24 -10129 Torino – Italy
Phone: +39.011.0906946
massimiliana.carello@polito.it

Simone Reitano
simone.reitano@polito.it

Lorenzo Sisca
lorenzo.sisca@polito.it

Henrique de Carvalho Pinheiro
henrique.decarvalho@polito.it

Alessandro Messana
alessandro.messana@polito.it

Alessandro Ferraris

alessandro.ferraris@polito.it

Andrea Airale
andrea.airale@polito.it

Acknowledgments

The authors would like to thank Phisik Instrumente (PI) GmbH & Co. KG - Germany for the support with the DuraAct piezoelectric transducers.

Definitions/Abbreviations

SHM	Structural Health Monitoring
Piezo	Piezoelectric Transducer
NDT	Non-Destructive Testing
GRP	Glass Reinforced Plastic